Inorg. Chem. **2009**, *48*, 1836−1843

An Efficient Homogeneous Intermolecular Rhenium-Based Photocatalytic System for the Production of H_2

Benjamin Probst,[†] Christoph Kolano,[‡] Peter Hamm,*[,‡] and Roger Alberto*[,†]

Institute of Inorganic Chemistry, University of Zürich, Winterthurerstrasse 190, CH-8057 Zürich Switzerland, and Institute of Physical Chemistry, University of Zürich, Winterthurerstrasse 190, CH-8057 Zürich Switzerland

Received July 16, 2008

We present an artificial photocatalytic model for photosystem I (PSI) using [ReBr(CO)$_3$bipy)] (**1**) as a photosensitizer, [Co(dmgH)$_2$] (**2**) as a *hydrogen evolution reaction* catalyst, and triethanolamine as an irreversible reductive quencher. Complex **1** is more robust in the long run, and turnover numbers were more than doubled in the present study as compared to the commonly used photosensitizer $[Ru(bipy)_3]^{2+}$. The quantum yield for hydrogen production with **1** was found to be 26 ± 2% (H produced per absorbed photon). Forward electron transfer between $\mathbf{1}^-$ and **2** was found to occur at a rate close to diffusion control ($k_1 = 2.5 \pm 0.1 \times 10^8$ M^{-1} s^{-1}). The rate of hydrogen production exhibited a linear dependence on the photon flux and a quadratic dependence on the total concentration of Co ($k_{obs} = 3.7 \pm 0.1$ M^{-1} s^{-1}). Therefore, a second-order process in Co^{III}−H is proposed. The process showed a complex dependence on [AcOH]. An excess of dimethylglyoxime was systematically added to the system to ensure the complete formation of **2** and reduce the portion of free $[Co]_{solv}^{2+}$, an efficient quencher of the excited state of **1**.

Introduction

The energy supply of our modern society largely depends on fossil fuels. As is nowadays accepted, reserves of fossil fuels decrease while consumption steadily increases. Concerns about the influence of greenhouse gases on earth's climate are furthermore not in favor of using large amounts of fossil fuels in the future. Alternative and sustainable energy sources are not sufficiently developed to compensate for fossil fuels. This holds especially for use in transportation (land, air, and sea) and for energy storage. The main discussions focus nowadays on dihydrogen (H_2) or methanol (MeOH) as viable alternatives. Great efforts are being undertaken for the development of fuel cells running with H_2 or MeOH as well as for the development of efficient storage for H_2.[1,2] This technology is more extensively developed, but the production of H_2 from fossil fuels remains a drawback (from today's 65 million tons a year, 48% is derived from natural gas, 30% from refinery/chemical offgases, 18% from coal, and 4% is produced electrochemically).[3]

The chemical storage of sunlight in H_2 by electrolysis using light-generated electrical energy is at an advanced state but remains inefficient. Alternatively, a direct conversion of sunlight into O_2 and H_2 would be a viable route in areas of high radiant flux, producing a fuel of high energy content which can be transported to metropolitan areas and converted to work and H_2O.

Since the late 1970s, remarkable results on artificial photosynthesis have been published, still setting today's benchmark. Brown et al. investigated photocatalytic water reduction with $[Ru(bipy)_3]^{2+}$ as a photosensitizer and macrocyclic cobalt complexes as catalysts for the *hydrogen evolving reaction* (*her*).[4] Efforts led by Lehn contributed substantial research both in H_2O oxidation[5] and reduction[6]

* To whom correspondence should be addressed. E-mail: ariel@aci.uzh.ch.
[†] Institute of Inorganic Chemistry.
[‡] Institute of Physical Chemistry.

(1) Armaroli, N.; Balzani, V. *Angew. Chem.* **2007**, *119*, 52–67.
(2) Olah, G. A. *Angew. Chem., Int. Ed.* **2005**, *44*, 2636–2639.
(3) Simbolotti, G. *Hydrogen Production & Distribution*; IEA: Paris, 2007.
(4) Brown, G. M.; Brunschwig, B. S.; Creutz, C.; Endicott, J. F.; Sutin, N. *J. Am. Chem. Soc.* **1979**, *101*, 1298–1300.
(5) Lehn, J. M.; Sauvage, J. P.; Ziessel, R. *New J. Chem.* **1979**, *3*, 423–427.
(6) Hawecker, J.; Lehn, J. M.; Ziessel, R. *New J. Chem.* **1983**, *7*, 271–277.
(7) Hawecker, J.; Lehn, J. M.; Ziessel, R. *Helv. Chim. Acta* **1986**, *69*, 1990–2012.

10.1021/ic8013255 CCC: $40.75
Published on Web 01/27/2009

Scheme 1. General Scheme for Photoreduction of H^+ by Light and an Irreversible Electron Donor, as Proposed by Lehn et al. (PS is $[Ru(bipy)_3]^{2+}$, D is triethanolamine, HA is the acid)[6]

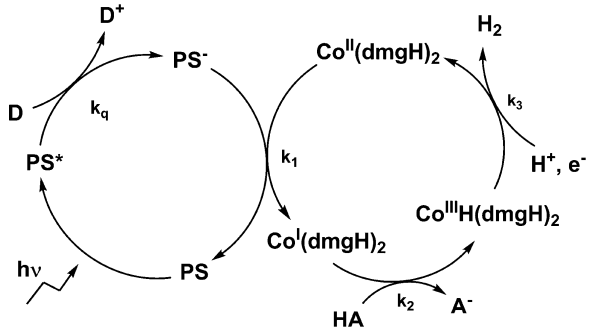

and in $CO_2 \rightarrow CO$ conversion.[7] Recent years have seen a revival of artificial photosynthesis, mainly employing the $[Ru(bipy)_3]^{2+}$ photosensitizer and noble metal catalysts to achieve proton reduction, the sacrificial electron donor mostly being a tertiary amine.[8−11] Lei et al. questioned the homogeneous character of these reactions, as they found H_2 production to correlate with colloid formation.[11] Rosenthal et al. studied systems involving rhodium-based dinuclear complexes,[12] and Fihri et al. studied systems involving heterodinuclear ruthenium−cobalt complexes.[13] Eisenberg used a platinum terpyridyl sensitizer in combination with cobalt dimethylglyoxime analogues,[14] and Bernhard used a series of iridium phenylpyridine sensitizers with rhodium *her* catalysts for photocatalytic homogeneous H_2 production.[15]

The vast majority of studies for photocatalytic H_2 production employed $[Ru(bipy)_3]^{2+}$ or derivatives as photosensitizers. The pioneering work by Lehn and co-workers showed that $[Ru(bipy)_3]^{2+}$, $[Co(dmgH)_2(OH_2)_2]$ (Co(II)-bisdimethylglyoxime-bisaquo) as a *her* catalyst, and triethanolamine as an irreversible electron donor in DMF produced H_2 under irradiation with light.[6] The principle of this dyad system, as proposed by the authors, is given in Scheme 1.

A drawback of this system was long-term stability, since after 10 h of irradiation, the rate of H_2 evolution decreased considerably. This was shown to be due to the decomposition of the sensitizer $[Ru(bipy)_3]^{2+}$. A substantial excess of dimethylglyoxime ($dmgH_2$) was required to increase the catalytic turnover. In the long run, tertiary amines as irreversible electron donors have to be replaced as well. A detailed mechanism of a similar system using $[Co(dmgH)_2]$ as a *her* catalyst and Et_3NH^+ as a proton source was provided by Razavet et al.[16] They showed by cyclic voltametry that H_2 production occurred by protonation of a $Co^{III}-H$ species (first-order in $Co^{III}-H$) with $k_{1.order} = 3 \times 10^2\ M^{-1}\ s^{-1}$ in DMF. In an electrochemical study, a second-order process in $Co^{III}-H$ with $k_{2.order} \approx 1 \times 10^6\ M^{-1}\ s^{-1}$ was observed in similar systems with $[Co(dmgBF_2)_2(CH_3CN)_2]$ as a catalyst in CH_3CN.[17] In a spectroscopic study in protic solvents, where $[HCo(dmgH)_2P(n\text{-}C_4H_9)_3]$ was employed as a *her* catalyst, a mixed mechanism with $k_{1.order} = 3.4 \times 10^4\ M^{-1}\ s^{-1}$ and $k_{2.order} = 4.2 \times 10^{-1}\ M^{-1}\ s^{-1}$ was reported.[18]

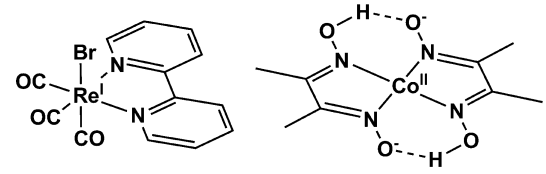

Thus far, most of the photocatalytic studies have employed $[Ru(bipy)_3]^{2+}$ as a photosensitizer.[4−6,8−10,13] Photocatalytic $CO_2 \rightarrow CO$ conversion catalyzed by $[ReBr(CO)_3bipy]$ (**1**) was published.[7,19−22] Heterodinuclear Ru−Re/ Zn−Re complexes, increasing the overlap with the solar spectrum, were reported for CO_2 reduction.[23−25] Reports about photocatalytic H_2 evolution with **1** are however rare. We, and later others, reported the influence of the axial ligand X in $[ReX(CO)_3bipy]$ for $CO_2 \rightarrow CO$ conversion.[19,26]

As shown in $[Ru(bipy)_3]^{2+}$ sensitized homogeneous systems, $[Co(dmgH)_2]$ (**2**) is a good choice for the reductive catalyst in *her*. Compound **2** is cheap, displays a low overpotential for proton reduction (30 mV) under neutral conditions, and achieves high turnover numbers.[16] The combination of **1** and **2** for photocatalytic H_2 production has, to the best of our knowledge, not yet been reported but is an important extension on the way to an improved system. We wish to present a detailed mechanistic and kinetic study for the photocatalytic production of H_2 in a homogeneous solution of **1** and **2** with triethanolamine (TEOA) as an irreversible electron donor. It turned out that the combination of rhenium complexes as photosensitizers and cobalt as a *her* catalyst is superior over the ruthenium−cobalt combination with respect to long-term performance.

(8) Ozawa, H.; Haga, M. A.; Sakai, K. *J. Am. Chem. Soc.* **2006**, *128*, 4926–4927.
(9) Rau, S.; Schafer, B.; Gleich, D.; Anders, E.; Rudolph, M.; Friedrich, M.; Gorls, H.; Henry, W.; Vos, J. G. *Angew. Chem., Int. Ed.* **2006**, *45*, 6215–6218.
(10) Elvington, M.; Brown, J.; Arachchige, S. M.; Brewer, K. J. *J. Am. Chem. Soc.* **2007**, *129*, 10644–10645.
(11) Lei, P.; Hedlund, M.; Lomoth, R.; Rensmo, H.; Johansson, O.; Hammarstrom, L. *J. Am. Chem. Soc.* **2008**, *130*, 26–27.
(12) Rosenthal, J.; Bachman, J.; Dempsey, J. L.; Esswein, A. J.; Gray, T. G.; Hodgkiss, J. M.; Manke, D. R.; Luckett, T. D.; Pistorio, B. J.; Veige, A. S.; Nocera, D. G. *Coord. Chem. Rev.* **2005**, *249*, 1316–1326.
(13) Fihri, A.; Artero, V.; Razavet, M.; Baffert, C.; Leibl, W.; Fontecave, M. *Angew. Chem., Int. Ed.* **2008**, *47*, 564–567.
(14) Du, P. W.; Knowles, K.; Eisenberg, R. *J. Am. Chem. Soc.* **2008**, *130*, 12576–12577.
(15) Cline, E. D.; Adamson, S. E.; Bernhard, S. *Inorg. Chem.* **2008**, *47*, 10378–10388.
(16) Razavet, M.; Artero, V.; Fontecave, M. *Inorg. Chem.* **2005**, *44*, 4786–4795.
(17) Hu, X.; Brunschwig, B. S.; Peters, J. C. *J. Am. Chem. Soc.* **2007**, *129*, 8988–8998.
(18) Chao, T. H.; Espenson, J. H. *J. Am. Chem. Soc.* **1978**, *100*, 129–133.
(19) Takeda, H.; Koike, K.; Inoue, H.; Ishitani, O. *J. Am. Chem. Soc.* **2008**, *130*, 2023–2031.
(20) Kutal, C.; Weber, M. A.; Ferraudi, G.; Geiger, D. *Organometallics* **1985**, *4*, 2161–2166.
(21) Hayashi, Y.; Kita, S.; Brunschwig, B. S.; Fujita, E. *J. Am. Chem. Soc.* **2003**, *125*, 11976–11987.
(22) Johnson, F. P. A.; George, M. W.; Hartl, F.; Turner, J. J. *Organometallics* **1996**, *15*, 3374–3387.
(23) Kiyosawa, K.; Masui, D.; Shimada, T.; Takagi, S.; Ishitani, O.; Inoue, H. *XXII IUPAC Symposium on Photochemistry*, Göteborg, Sweden, 2008.
(24) Sato, S.; Koike, K.; Inoue, H.; Ishitani, O. *Photochem. Photobiol. Sci.* **2007**, *6*, 454–461.
(25) Gholamkhass, B.; Mametsuka, H.; Koike, K.; Tanabe, T.; Furue, M.; Ishitani, O. *Inorg. Chem.* **2005**, *44*, 2326–2336.
(26) Kurz, P.; Probst, B.; Spingler, B.; Alberto, R. *Eur. J. Inorg. Chem.* **2006**, *296*, 6–2974.

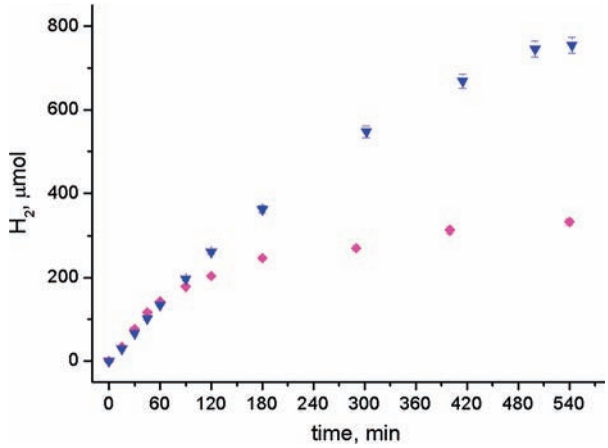

Figure 1. Comparison between $[ReBr(CO)_3bipy]$ (▼) and $[Ru(bipy)_3]^{2+}$ (♦) chromophores (0.5 mM in **1** and $[Ru(bipy)_3]^{2+}$ respectively, 1 mM $Co(OAc)_2 \cdot 4H_2O$, 6 mM $dmgH_2$, 1 M TEOA, 0.1 M AcOH, DMF, Argon).

Results and Discussion

To obtain detailed insight into the mechanism of H_2 production, the rate constants of the different elementary reaction steps, as shown in Scheme 1, were the focus of our study. Besides qualitative long-term stability as compared to the $[Ru(bipy)_3]^{2+}-[Co(dmgH)_2]$ system,[6] we investigated the influence of excess $dmgH_2$, [AcOH], photon flux and quantum yields, rate, and mechanism on the final H_2 evolution step.

The main methods employed are hydrogen measurements under continuous wave irradiation to determine dependencies of the composition of the system on dH_2/dt. On the other hand, time-resolved IR spectroscopy provided a tool for the study of the initial phase of the *her*, namely, the rhenium cycle.

1. Rhenium Cycle. Catalytic Performance. $[Ru(bipy)_3]^{2+}$ has been described as being moderately stable with respect to long-term performance.[6] In a first step, we qualitatively compared the rate of H_2 production under identical conditions for $[Ru(bipy)_3]^{2+}$ and **1**. A time-dependent comparison is given in Figure 1. When subjected to photolysis ($h\nu \geq 400$ nm), the two chromophores **1** and $[Ru(bipy)_3]^{2+}$ performed equally well in an initial phase of the experiment for about 60 min. The rate of H_2 evolution was 3.7 ± 0.05 $\mu M\ s^{-1}$ for **1** and 4.1 ± 0.09 $\mu M\ s^{-1}$ for $[Ru(bipy)_3]^{2+}$. When subjected to photolysis for a longer time, **1** continued producing H_2, whereas the $[Ru(bipy)_3]^{2+}$ system substantially slowed down. After about 9 h of irradiation, more than twice the amount of H_2 was observed for **1** as compared to $[Ru(bipy)_3]^{2+}$. The turnover number (defined as H_2 per photosensitizer) for **1** and $[Ru(bipy)_3]^{2+}$ was 150 and 65, respectively. In fact, whereas the AcOH and TEOA concentrations could be considered as constant for the first 60 min, H^+ from acetic acid was consumed after 5 h and about 15% of the reductive quencher TEOA after 9 h. The addition of more equivalents of TEOA and AcOH after 5 h did not increase long-term performance. Qualitatively, both systems seemed to undergo some deactivation pathway, but **1** shows an improved long-term stability.

Scheme 2. General Representation of a Second-Order Pathway in $Co^{III}-H$ to Hydrogen[a]

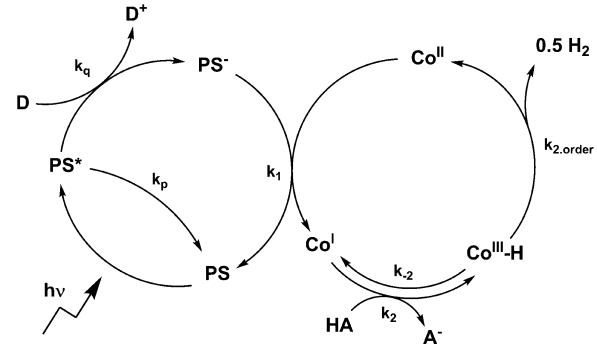

[a] PS represents the photosensitizer $[ReBr(CO)_3bipy]$. Co^{II} is $[Co^{II}(dmgH)_2]$. D is the donor TEOA, and HA is acetic acid.

Time-Resolved IR Spectroscopy. The first three reactions along the proposed catalytic cycle (k_{abs}, k_p, k_q, and k_1, Scheme 2) all involve the $[ReBr(CO)_3bipy]$ sensitizer in different electronic configurations (ground, excited, and reduced states). Time-resolved IR spectroscopy is therefore the method of choice for a kinetic analysis of this part of the system. The ground-state IR spectrum of **1** in DMF is shown in Figure 2a and exhibits strong and characteristic bands in the $1800-2100$ cm^{-1} region. The bands at 1897, 1918, and 2022 cm^{-1} have been assigned to a′(2) [asymmetric stretching of CO_{ax} and CO_{eq}], a″ [asymmetric stretching of CO_{eq}], and a′(1) [symmetric stretching of all CO's] modes, respectively. The photochemistry of **1** upon 400 nm excitation is well understood and has been described in detail.[21,27−33] Using an UV-pump−IR-probe setup[34] allowed us to follow the reaction from picoseconds to microseconds and to unravel the rate-limiting step. Our DFT calculations (B3LYP) at the LANL2DZ level of theory and previous experiments[28] showed that upon excitation or reductive quenching the symmetric and asymmetric set of CO stretching frequencies will undergo characteristic spectral shifts.

In a first series of experiments, we investigated the photochemistry of a 1 mM solution of **1** in degassed DMF upon 400 nm excitation. Within the response time of our setup, we observed the instantaneous formation of a new set of symmetric and asymmetric CO stretching bands, which were shifted to higher wavenumbers. A singular value decomposition (SVD) analysis and a fit of kinetic traces at selected spectral positions yielded a lifetime of $\tau_{1/2} = 51$ ns

(27) Glyn, P.; George, M. W.; Hodges, P. M.; Turner, J. J. *J. Chem. Soc., Chem. Commun.* **1989**, 1655–1657.
(28) George, M. W.; Johnson, F. P. A.; Westwell, J. R.; Hodges, P. M.; Turner, J. J. *J. Chem. Soc., Dalton Trans.* **1993**, 2977–2979.
(29) Turner, J. J.; George, M. W.; Johnson, F. P. A.; Westwell, J. R. *Coord. Chem. Rev.* **1993**, *125*, 101–114.
(30) Stufkens, D.; Vlcek, A. *Coord. Chem. Rev.* **1998**, *177*, 127–179.
(31) Bredenbeck, J.; Helbing, J.; Hamm, P. *J. Am. Chem. Soc.* **2004**, *126*, 990–991.
(32) Vlcek, A.; Busby, M. *Coord. Chem. Rev.* **2006**, *250*, 1755–1762.
(33) Busby, M.; Matousek, P.; Towrie, M.; Vlcek, A. *Inorg. Chim. Acta* **2007**, *360*, 885–896.
(34) Bredenbeck, J.; Helbing, J.; Hamm, P. *Rev. Sci. Instrum.* **2004**, *75*, 4462–4466.

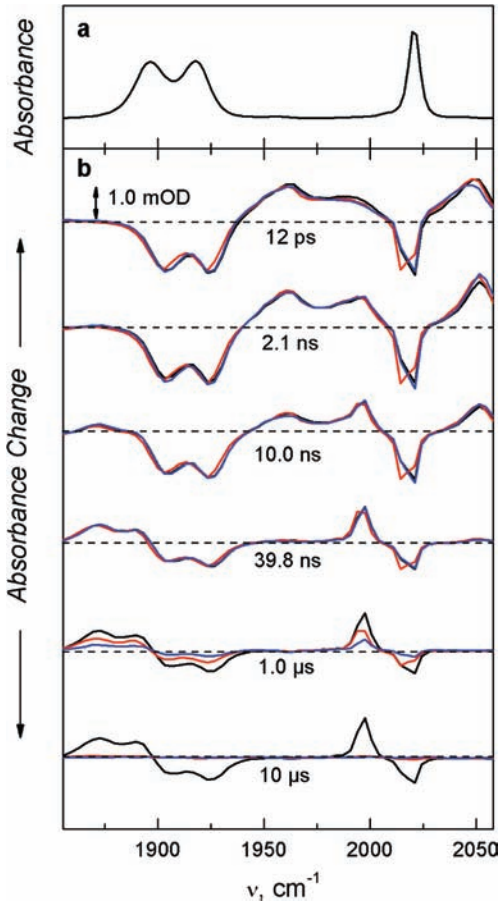

Figure 2. (a) FTIR spectrum of a 1 mM solution of **1** containing 1 M TEOA in degassed DMF (spectral resolution 2 cm^{-1}). (b) Magic angle pump−probe spectra (1 mM **1**, 1 M TEOA, 0.1 M AcOH, degassed DMF, spectral resolution 3.5 cm^{-1}) at different time delays after excitation at λ_{ex} = 400 nm. Bands appearing upon irradiation are pointing upward; bands disappearing are pointing downward. Black spectra, 0 mM of **2**; red spectra, 2 mM of **2**; blue spectra, 5 mM of **2**.

for this transient species. We assigned this transient species to the excited state of **1** (designated as ^{3}MLCT), in agreement with previous experiments,[20,28,30] reporting that the shift to higher wavenumbers is caused by a formal Re^{II} center coordinated to the bpy radical anion.

When the experiment was performed in the presence of an electron donor (1 M TEOA), a new, second transient evolved from the ^{3}MLCT state on a time scale of ∼15 ns and remained constant for 10 μs, the maximum delay time of our setup (Figure 2b, 0 mM [$Co(dmgH)_2$], black spectrum). This lifetime is in good agreement with Stern−Volmer plots of luminescence intensities for **1** as a function of the TEOA concentration ($k_q = 6 \times 10^7$ M^{-1} s^{-1}).[20,26,35] The observed second transient gave rise to a new set of symmetric and asymmetric CO stretching bands, which were now red-shifted. We assign this transient to the reduced form $\mathbf{1}^-$. Accordingly, this assignment was consistent with a red shift of the corresponding set of $\nu_{C=O}$ vibrations. This was to be expected for a formally reduced 2,2′-bipyridine ligand coordinated to a Re^I center.[28] Together, $\tau_{1/2}$ and k_q would predict a quenching yield of 0.78 ± 0.04 according to eq 1.

(35) Luong, J. C.; Nadjo, L.; Wrighton, M. S. *J. Am. Chem. Soc.* **1978**, *100*, 5790–5795.

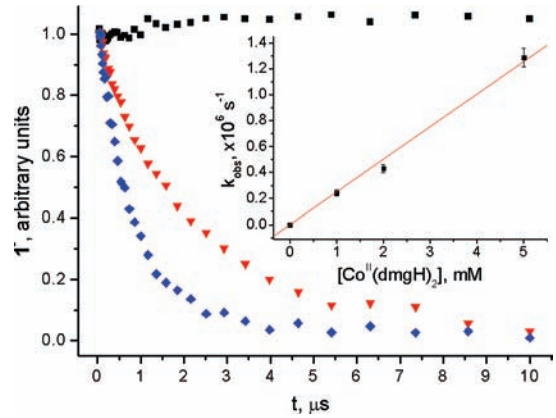

Figure 3. Transient kinetic traces for $\mathbf{1}^-$, monitored at ($\tilde{\nu}$) = 1997.5 cm^{-1}, in the presence of different cobalt concentrations (■, 0 mM of **2**; ▼, 2 mM of **2**; ♦, 5 mM of **2**). Inset: Decay rate of $\mathbf{1}^-$ as a function of $[Co]_{tot}$. The plot of k_{obs} vs concentration of **2** yields the rate for the forward electron transfer reaction ($\mathbf{1}^- + \mathbf{2} \rightarrow \mathbf{1} + [Co^I(dmgH)_2]^-$).

On the other hand, if we compare the intensities of the bleaching (negative) bands of the Re complex during the lifetime of the ^{3}MLCT state (10 ps to 10 ns) with that after the reductive quenching (Figure 2b), we estimate a yield of $\Phi_{red} \approx 0.3$. This analysis assumes that the vibrational bands of the unpumped Re complex are spectrally well separated from that of transient photoproducts (which is the case). In this case, the early bleach intensity is a direct measure of the number of molecules initially excited into the ^{3}MLCT state, whereas at later delay times it is a measure of the number of molecules that have not reacted back to the ground state. Obviously, the ^{3}MLCT of **1** was quenched in a nonproductive (∼60%) and in a reductive (∼40%) fashion on the same time scale, indicative of a cage escape yield of $\Phi_{cage} \approx 0.4$.

$$\Phi_q = \frac{k_q[\text{TEOA}]}{k_q[\text{TEOA}] + \tau_{1/2}^{-1}}, \quad \Phi_{red} = \Phi_q \Phi_{cage} \qquad (1)$$

In a next set of experiments, all of the components of the *her* system were combined and the spectra recorded in the presence of 1, 2, and 5 mM $Co(OAc)_2 \cdot 4H_2O$ and a 6-fold excess of $dmgH_2$ (Figure 2b, red and blue spectra). As can be seen in Figures 2b and 3, the signal for $\mathbf{1}^-$ was quenched depending on $[Co]_{tot}$. A fit of the kinetic traces at selected spectral positions (Figure 3) and a SVD analysis yielded lifetimes of 4.1 μs and 2.3 and 0.8 μs. The experimental C=O stretching vibrations of the observed species and the obtained global time constants are summarized in Table 1.

We estimated an upper limit for the concentration of $\mathbf{1}^-$ of 80 μM as calculated from the spectral overlap of **1** with a 400 nm laser pulse of 2.5 μJ. On the basis of this upper limit concentration, the kinetics were expected to be pseudo-first-order. Thus, for the forward electron transfer reaction between $\mathbf{1}^-$ and $[Co^{II}(dmgH)_2]$, as shown in the inset of Figure 3, a rate constant of $k_1 = 2.5 \pm 0.1 \times 10^8$ M^{-1} s^{-1} was obtained. This is about 5% of the diffusion-controlled rate in DMF containing 1 M TEOA according to the Stokes−Einstein−Smoluchowski equation ($k_{dc} \sim 5 \times 10^9$ M^{-1} s^{-1}). This value is well in agreement

Table 1. Global Time Constants and Experimental C≡O Stretching Vibrations of the Species Observed Here and as Compared to the Literature

	$\nu_{C=Osym}$ [cm^{-1}]	$\nu_{C=Oasym}$ [cm^{-1}]	$\nu_{C=Osym}$ [cm^{-1}], lit.	$\nu_{C=Oasym}$ [cm^{-1}], lit.	global time constant (decay)	global time constant (decay), lit.
1	2021.9	1896.5, 1917.7	2023[a]	1902, 1914[a]		
			2019[b]	1893, 1914[b]		
^{3}MLCT of **1**	2051.4	1960.5, 1997.5	2068[a]	1957, 1989[a]	51.1 ± 1.3 ns	30 ns,[a] 50 ns,[b] 55 ns[d]
			2064[c]	1957, 1987[c]		
1$^-$	1997.5	1872.9, 1889.8	1998[a]	1866, 1880[a]	15.4 ± 0.2 ns (formation)	>10 ms[a] (decay)
			1994[b]	1862, 1880[b]	>10 μs (decay)	>200 ms[b] (decay)
1$^-$ (1 mM of **2**)					4.1 ± 0.4 μs	
1$^-$ (2 mM of **2**)					2.3 ± 0.2 μs	
1$^-$ (5 mM of **2**)					0.78 ± 0.04 μs	

[a] Data measured for $ReCl(CO)_3bipy$ in MeCN.[21] [b] Data measured for $ReCl(CO)_3bipy$ in DMF.[28] [c] Data measured for $ReCl(CO)_3bipy$ in CH_2Cl_2.[28] [d] Data measured for $ReBr(CO)_3bipy$ in DMF.[20]

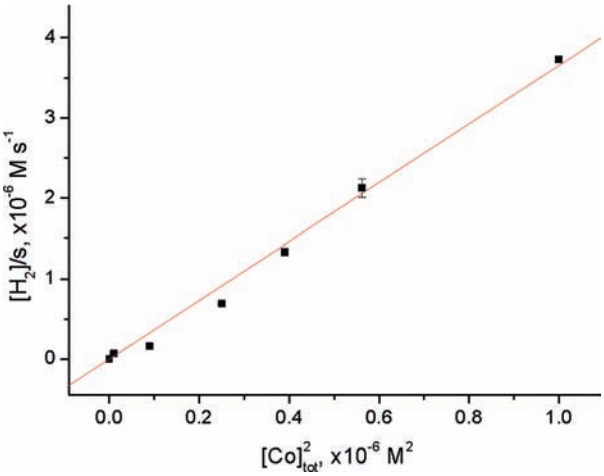

Figure 4. H_2 production rates as a function of $[Co]^2_{tot}$. An excess of 6 equiv of $dmgH_2$ was used per cobalt, 0.5 mM **1**, 1 M TEOA, 0.1 M AcOH, DMF, and argon.

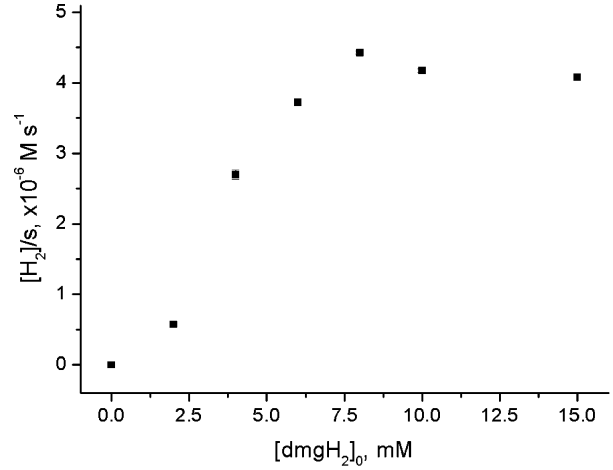

Figure 5. Initial turnover frequency as a function of $dmgH_2$ (0.5 mM **1**, 1 mM $Co(OAc)_2 \cdot 4H_2O$, 1 M TEOA, 0.1 M AcOH, DMF, and argon).

with results of a laser flash photolysis study for the forward electron transfer between $[Ru(bipy)_3]^+$ and $[Co^{II}(Me_6[14]dieneN_4)]^{2+}$ ($k = 1.8 \times 10^8$ M^{-1} s^{-1}) in a $Eu^{2+}/[Ru(bipy)_3]^{2+}/[Co^{II}(Me_6[14]dieneN_4)]^{2+}/H_2O/HCl$ system.[4]

2. Cobalt Cycle. Cobalt Dependence. The initial rate of H_2 formation as a function of the total Co concentration, $[Co]_{tot}$, should elucidate whether the major pathway was first- or second-order in cobalt. Accordingly, $[Co]_{tot}$ was varied while all of the other parameters were kept constant. For a first-order process, we expected a linear dependence since AcOH was constant over a time period of 120 min. We observed a marked dependence of the H_2 production rate on the total cobalt concentration (Figure 4). An excess of 6 equiv of $dmgH_2$ per cobalt was applied in order to keep the concentration of **2** constant (vide infra). The rate of H_2 production was found to have a square dependence on $[Co]_{tot}$, as is obvious from a corresponding linearization of the original curve. The observed second-order rate constant was $k_{obs} = 3.7 \pm 0.10$ M^{-1} s^{-1}. This square dependence implies hydrogen formation via a path second-order in $Co^{III}-H$ as is argued in the discussion and depicted in eq 5. Further increase of the cobalt concentration above 1 mM gave a constant rate of H_2 formation at about 3.75 μM s^{-1} (Supporting Information 1). We assume that at this concentration the photon flux became rate-limiting (see the Limiting Processes section).

Cobalt/dmgH$_2$ Ratio. One of the critical factors in the **1**−**2** system is the role of $dmgH_2$. As noted by Hawecker et al., an excess of $dmgH_2$ was required to achieve reasonable performance.[6] The overall stability constant (log β) for the formation of **2** from $[Co]_{solv}^{2+}$ and $dmgH_2$ has been reported to be in the range of 20 for a 1:1 dioxane−water mixture as determined by potentiometric titration.[36,37] The dependence of the H_2 formation rate as a function of $dmgH_2$ concentration confirmed that the initial turnover frequency of the system increased considerably with increasing $[dmgH_2]$ while keeping all other parameters constant. A plateau of about 4 μM s^{-1} H_2 was reached at 7.5 equiv of $dmgH_2$ per cobalt (Figure 5).

Complex **2** seemed to be less stable than expected. We found, in an electrochemical study, a conditional stability constant of $\beta_{cond.} \approx 10^6$ M^{-2} (eq 2, Supporting Information 2). The discrepancy to the literature value of $\log(\beta) = 20$ can be explained by the different solvent system used and the different definition of β. Accordingly, **2** was formed almost quantitatively upon the addition of 6 equiv of free ligand per cobalt as used in our photolysis experiments (95%). $[Co]_{solv}^{2+}$ should not interfere with excitation, quenching, and electron transfer. It is, however, known from other

(36) Freiser, H. *Analyst* **1952**, *77*, 830–845.
(37) Banks, C. V.; Anderson, S. *Inorg. Chem.* **1963**, *2*, 112–115.

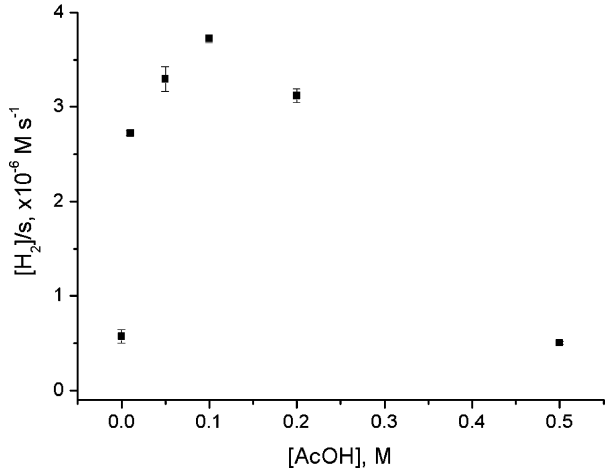

Figure 6. Dependence of hydrogen production rate on acid concentration (0.5 mM 1, 1 mM $Co(OAc)_2$, 6 mM $dmgH_2$, 1 M TEOA, DMF, and argon).

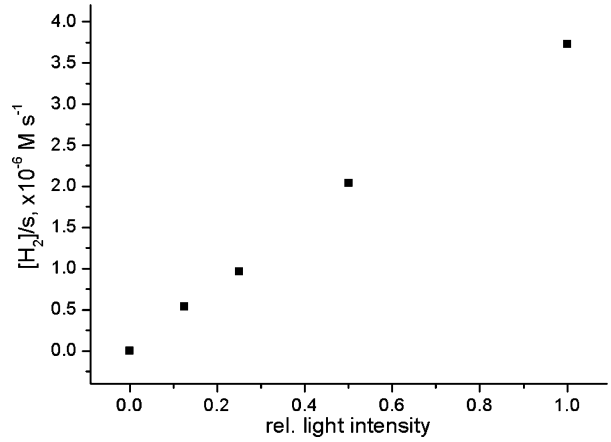

Figure 7. Variation of photon flux versus $[H_2]$/s (0.5 mM **1**, 1 mM **2**, 1 M TEOA, 0.1 M AcOH, DMF, and argon).

systems that paramagnetic cations rapidly quench triplet excited states (triplet−triplet quenching).[38] We investigated by Stern−Volmer fluorescence quenching whether $[Co]_{solv}^{2+}$ would act in the same way. We found that $[Co]_{solv}^{2+}$, added to the system in the form of $[Co(OAc)_2]$, efficiently quenched the excited state of **1** with $k_q = 2.57 \pm 0.07 \times 10^9\ M^{-1}\ s^{-1}$ (Supporting Information 3) in the absence of $dmgH_2$. Thus, an excess of $dmgH_2$ was required to optimize the amount of active *her* catalyst but also, more importantly, to avoid the presence of $[Co]_{solv}^{2+}$ since it abolished the H_2 formation process efficiently and at a rate which is close to diffusion control.

$$\beta_{cond} = \frac{[Co^{II}(dmgH)_2]}{[Co^{II}_{solv}][dmgH_2]^2} \qquad (2)$$

Dependence on Acidity. A further parameter in the system was the pH value. Although pH is difficult to define in a nonaqueous solution, the amount of added protons in the form of acetic acid might be representative for the amount of immediately available protons. We varied the concentration of acetic acid in the system while keeping the other parameters constant. In particular, the concentration of TEOA was not altered and remained constant at 1 M. The rate dependence on acetic acid concentration is shown in Figure 6.

Not surprisingly, a strong acetic acid concentration dependence on the formation rate of H_2 was found reaching a maximum at about 0.1 M acetic acid in 1 M TEOA ($3.72 \pm 0.04\ \mu M\ s^{-1}$). Interestingly, catalysis also took place without any acetic acid, although at a very slow rate ($0.57 \pm 0.07\ \mu M\ s^{-1}$). It is likely that residual protons coming from water in the system and the decomposition of TEOA[39] were responsible for this process. In the presence of 0.05 M water instead of acetic acid, the hydrogen production rate was $0.70 \pm 0.02\ \mu M\ s^{-1}$. Below and above 0.1 M, respectively, two processes decrease the H_2 production rate. The decrease observed at a high acetic acid concentration is likely to be caused by the instability of **2** at a high acid concentration, resulting in the generation of the quencher $[Co]_{solv}^{2+}$ as described before.[16] This is supported by the observation that at a low acetic acid concentration the system performed at a more constant rate over a long period of time. At a low acid concentration, the protonation of Co^I might have become limiting as acetic acid enters the overall equation.

3. Performance of the System. Quantum Yield. The photon flux was varied systematically in a series of experiments to study its influence on the hydrogen production rate. It was found to correlate linearly with hydrogen production at 1 mM **2** (Figure 7), indicating that the photon flux is rate-limiting under these conditions. The overall quantum yield of hydrogen production (0.5 H_2 per absorbed photon) was $26 \pm 2\%$ at 415 nm (see the Experimental Section) in this regime. This value was confirmed independently (within error) by ferrioxalat actinometry. Quantum yields in this range are well in accordance with literature reports on similar systems.[40] It has to be kept in mind though that the actual quantum yield might be smaller due to the generation of a second reducing equivalent by the decomposition process of TEOA.[39,41] The time-resolved experiments suggest (Figure 2) that the dominant contribution in limiting the overall quantum yield is the first electron transfer step, that is, the reductive quenching of the initially excited ^{3}MLCT state of the Re complex.

Limiting Processes. According to these observations, two rate-limiting factors for the Re−Co system were obvious. A second-order process in cobalt was the rate-limiting step when $[Co]_{tot}$ was in the range of 0−1 mM. By exceeding this concentration of *her* catalyst **2**, the photon flux became rate-limiting (Supporting Information 1). To confirm this conclusion, the rate of H_2 formation should no longer linearly depend on the photon flux at a concentration of **2** < 1 mM. Thus, we performed the same experiments as above and fixed the $[Co]_{tot}$ at 0.5 mM. The rate-limiting step changed from

(38) Porter, G.; Wright, M. R. *Discuss. Faraday Soc.* **1959**, 18–20.
(39) Kalyanasundaram, K. *J. Chem. Soc., Faraday Trans.* **1986**, *82*, 2401–2415.
(40) Sutin, N.; Creutz, C.; Fujita, E. *Comments Inorg. Chem.* **1997**, *19*, 67–92.
(41) Kutal, C.; Corbin, A. J.; Ferraudi, G. *Organometallics* **1987**, *6*, 553–557.

photon flux (at low photon flux) to a second-order process in cobalt (at high photon flux; Supporting Information 5).

Homogeneity. It has been noted for similar systems, using late transition metals as *her* catalysts, that hydrogen production correlated with colloid formation during irradiation.[11,42] On the basis of the kinetic results presented here, namely, the second-order dependence on cobalt, but also the dependence on $dmgH_2$ concentration and the fact that Co^I was produced, which is known to undergo the proposed reaction series, colloid formation as a main source of hydrogen seemed unlikely. Nevertheless, we probed a standard experiment (0.5 mM **1**, 1 mM **2**, 1 M TEOA, 0.1 M AcOH, DMF, Ar) at varying irradiation times for colloid formation by light scattering (see Supporting Information 6). The results clearly showed that, during 6 h of irradiation, no significant amounts of colloids (particle sizes from 0.5 to 1000 nm) were produced.

4. Discussion. The elucidation of essential parameters in the Re−Co system for photocatalytic H_2 formation showed that **1** is a viable alternative for $[Ru(bipy)_3]^{2+}$ used in similar experiments.[4,6,13,40] The long-term performance of **1** in particular is superior over that of $[Ru(bipy)_3]^{2+}$. Our time-resolved data unambiguously show that reductive quenching is the first step for the present system. The overall quantum yield is about 25%; however, the time-resolved measurements suggest that the dominating loss occurs during the reductive quenching of the ^{3}MLCT state of the Re complex. Further investigations elucidated the rate-controlling step. The forward electron transfer rate between $\mathbf{1}^-$ and **2** was $k_1 = 2.5 \pm 0.1 \times 10^8\ M^{-1}\ s^{-1}$ and was therefore not rate-controlling. Under mild conditions (e.g., solar irradiation), photon flux will limit the overall process. On the other hand, we could show that a second-order process in cobalt with a conditional rate constant of $k_{obs} = 3.7 \pm 0.1\ M^{-1}\ s^{-1}$ limited the rate, provided that the photon flux was high enough (Figure 4). In principle, two pathways to hydrogen can be followed after the protonation of Co^I (eq 3): either a first-order (eq 4) or a second-order process in $Co^{III}-H$ (eq 5).

$$Co^I + HA \rightarrow Co^{III}-H + A^- \ (K_2, k_2) \quad (3)$$

$$Co^{III}-H + HA \rightarrow Co^{III} + H_2 + A^- \ (k_{1.order}) \quad (4)$$

$$2Co^{III}-H \rightarrow 2Co^{II} + H_2 \ (k_{2.order}) \quad (5)$$

Hu et al. demonstrate in their investigation that, for a second-order process, if the protonation of Co^I is fast (k_2), a square dependence of dH_2/dt on Co^I is found (eq 6).[17]

$$\frac{d[H_2]}{dt} = K_2^{\,2} k_{2.order} \left[\frac{[Co^I][HA]}{[A^-]}\right]^2 \quad (6)$$

This indicates that in the present system H_2 was formed by the reaction of two $Co^{III}-H$'s and not by the protonation of the latter, as observed elsewhere.[16]

Scheme 2 summarizes the complete picture of the system under study. Thermodynamics should favor the second-order route to H_2, but kinetic reasons might favor the first-order process.[43] We believe that parallel mechanisms occur, depending on the concentration of $Co^{III}-H$, the concentration of the added acid, and its pK_a. In contrast to this Re−Co system, Razavet et al. found in an electrochemical system with **2** in DMF and $[Et_3NH]Cl$ as a H^+ donor a first-order process to H_2 with $k_2 = 10^4\ M^{-1}\ s^{-1}$ and $k_{1.order} = 300\ M^{-1}\ s^{-1}$.[16] This mechanism might result from the different acids ($[Et_3NH]Cl$ vs AcOH) and solvent mixtures in their experiments. Obviously both Et_3NH^+ and AcOH are acids strong enough to protonate Co^I, but only Et_3NH^+ also protonates $Co^{III}-H$ (pK_a $Et_3NH^+ = 9.2$, AcOH = 13−14, in DMF).[44] Hu et al. found in an electrochemical study with $[Co^{II}(dmgBF_2)(MeCN)_2]$ as a *her* catalyst a predominant second-order route to H_2 with $k_{2.order} \approx 10^6\ M^{-1}\ s^{-1}$, using CF_3COOH ($pK_a = 12.7$), $Et_2O{\cdot}HCl$ ($pK_a = 8.9$), and other acids.[17,45] Chao et al. reported in a spectroscopic study with $[HCo^{III}(dmgH)_2P(n\text{-}C_4H_9)_3]$ in protic solvents a mixed first-/second-order process with $k_{2.order} = 3.4 \times 10^4\ M^{-1}\ s^{-1}$.[18] A detailed mechanistic analysis or a simulation might unravel the single components that contribute to k_{obs} in this study.

Conclusion

We presented in this study a new photocatalytic system for the efficient production of H_2 with a quantum yield essentially limited by the quenching process of TEOA and the ^{3}MLCT of **1**. The system showed a much better overall performance than that of the widely studied Ru−Co system, which requires additional optimization. The detailed kinetic studies performed for the different elementary steps in our catalytic cycle revealed a second-order process in cobalt as the final H_2 releasing step. This fundamental result has strong implications for the rational design of future *her* catalysts. Further studies are on the way to fully elucidating the parameters that govern the cobalt cycle. Currently, we are working on improving stability and efficiency of the *her* catalyst by tuning its electronic and steric properties.

Experimental Section

All chemicals were of reagent grade and used without further purification. Spectroscopic-grade DMF was purchased from Acros. Electrochemical-grade $TBA[PF_6]$, $Co(OAc)_2{\cdot}4H_2O$, and $dmgH_2$ were purchased from Fluka. Water was doubly distilled before use. Synthetic reactions were carried out under N_2 or Ar using standard Schlenk techniques. The synthesis of **1** and $[Ru(bipy)_3]^{2+}$ has been described in the literature.[46,47]

Fluorescence measurements were performed on a Perkin-Elmer LS50B fluorescence spectrometer with argon-purged solution samples in 1 cm cells.

Electrochemical measurements were carried out in DMF containing 0.1 M $TBA[PF_6]$ as a conducting electrolyte. A Metrohm 757VA Computrace electrochemical analyzer was used with a

(42) Du, P.; Schneider, J.; Fan, L.; Zhao, W.; Patel, U.; Castellano, F. N.; Eisenberg, R. *J. Am. Chem. Soc.* **2008**, *130*, 5056–5058.
(43) Kellett, R. M.; Spiro, T. G. *Inorg. Chem.* **1985**, *24*, 2373–2377.
(44) Izutsu, K. *Acid-Base Dissociation Constants in Dipolar Aprotic Solvents*; Blackwell Scientific Publications: Oxford, 1990.
(45) Hu, X. L.; Cossairt, B. M.; Brunschwig, B. S.; Lewis, N. S.; Peters, J. C. *Chem. Comm.* **2005**, 4723–4725.
(46) Abel, E. W.; Wilkinson, G. *J. Chem. Soc.* **1959**, 1501–1505.
(47) Burstall, F. H. *J. Chem. Soc.* **1936**, 173–175.

standard three-electrode setup of glassy carbon working and Pt auxiliary electrodes and a Ag/AgCl reference electrode. All potentials are given versus Ag/AgCl (Fc/Fc^+ at +500 mV).

Light scattering was measured on a DynaPro Titan TC (Wyatt Technology). The sample was ultracentrifuged and probed by an 828 nm laser in either a 50 μL (not stirred) or 2 mL (stirred) cuvette after various irradiation times (25 °C, 90° to the probe beam, 100% laser power). Each measurement consisted of 20 acquisitions (10 s each).

Gas chromatograms were recorded using a Varian CP-3800 gas chromatograph with argon as the carrier gas and a 3 m × 2 mm molecular sieve 13X 80−100. The gas flow was set to 20 mL/min. The oven was operated isothermally at 100 °C. The 100 μL gas samples were injected using a Hamilton (1825 RN) gastight microliter syringe. The gases were detected using a thermal conductivity detector (Varian) operated at 150 °C. Calibrations were performed by the injection of known quantities of pure hydrogen diluted in the same Schlenk tube containing the same volume of DMF as used for the measurements.

Photochemical Measurements. Typical reactions were carried out in a 54 mL septum-capped Schlenk tube. Exact volumes were determined gravimetrically. A total of 10 mL of a solution containing the respective mixture in DMF was prepared, wrapped in black foil and degassed using an argon-purged Schlenk line. The mixture was equilibrated under 1.5 bar of argon pressure for 15 min and then transferred to a dark room for illumination. The light source was a Leica Pradovit S AF slide projector equipped with a 250 W Osram Xenophot HLX lamp. The light was filtered with a 400 nm cutoff filter (Schott GG 400, no transmission below 400 nm, spectra see Supporting Information 7, black) before reaching the sample at a 40 cm distance from the projector. If necessary, the radiant flux was cut in $(1/2)^n$ by using n neutral density filters (OD = 0.3). The 100 μL gas samples were drawn from the headspace above the solution and injected into the GC-TCD gas analyzer.

Quantum Yield Measurments. Light at 415 nm was produced by frequency-doubling a Spectra-Physics Tsunami femtosecond laser system. It was then focused (beam diameter ~ 5 mm) on a SUPRASIL quartz cell (Helma, 20 mm). The radiant flux through the sample was determined by an Ophir Laser Power Meter (Model AN/2) before and after the addition of the chromophore to calculate the number of absorbed photons. Headspace sampling for hydrogen detection at respective times was done as described above.

To obtain an independent verification of the quantum yield, we also performed actinometry using $K_3[Fe(ox)_3]$ as the chemical actinometer and a 300 W Xe arc lamp (LOT Oriel) in line with a water filter and a 400 nm bandpass filter (Andover Corporation, 400FS10-50, 402 nm).

UV-Pump−IR-Probe Spectroscopy. The system for UV-pump−IR-probe spectroscopy consists of two synchronized[34] commercially available Ti:sapphire-oscillator/regenerative amplifier femtosecond laser systems operating at 800 nm (Spectra Physics; duration, ~100 fs; repetition rate, 1 kHz; energy, ~600 μJ/pulse), allowing us to cover the time range from 2 ps to 10 μs. Laser system 1 was frequency-doubled with a BBO crystal. The obtained 400 nm pulses were subsequently focused into the sample cell (100 μm thick) with a spot size of ~200 μm diameter. Measurements were carried out using parallel and perpendicular polarized pump pulses generated by a computer-controlled half-wave plate, from which the magic angle signal was calculated. Laser system 2 pumped a white-light-seeded two-stage BBO optical parametric amplifier (OPA),[48] the signal and idler pulses of which were difference-frequency mixed in a $AgGaS_2$ crystal. They were separated into two parts to achieve broadband probe and reference pulses. These IR-probe pulses were focused into the sample cell in spatial overlap with the 400 nm pump pulse. The reference and probe pulses were dispersed in a monochromator (SPEX Triax Series) and imaged onto a 2 × 64 pixel MCT (Mercury Cadmium Telluride) detector array (InfraRed Associates Inc.), revealing a spectral resolution of 3.5 cm^{-1}. To ensure efficient exchange of the excited volume, the sample was pumped rapidly by a tubing pump (Ismatec BVP equipped with EasyLoad II pump-head, flow ~5.0 mL/min) to a small sealed reservoir (V ≈ 3 mL). The pressurized flow of the reservoir transferred the sample through the flow cell (path length 100 μm) and finally back to the tank, which was protected from light. Since TEOA is a very aggressive compound, the EasyLoad II pump-head was equipped with chemically resistant fluoroelastomer tubing from Gore (Chem-Sure; 1.6 mm ID, 1.6 mm wall, 4.8 mm o.d., 305 mm length). The concentration of the Re sample (**1**) in DMF (Acros, spectroscopic-grade) was adjusted to 1 mM, and the solution was purged with argon continuously. During the course of the measurement, unwanted photoproducts accumulated to less than 5%.

Acknowledgment. We thank Alexander Rodenberg for technical assistance in the quantum yield measurements. We are grateful to the Swiss National Science Foundation (SNF) for financially supporting this work (Grant No. 200021-119798).

Supporting Information Available: H_2 formation as a function of $[Co(dmgH)_2]$ and photon flux, stability constant determination for $[Co(dmgH)_2]$, luminescence quenching of **1** by Co^{2+}, light scattering experiments, and the spectra of the light sources used. This material is available free of charge via the Internet at http://pubs.acs.org.

IC8013255

(48) Hamm, P.; Kaindl, R. A.; Stenger, J. *Opt. Lett.* **2000**, *25*, 1798–1800.